Solid State Nuclear Magnetic Resonance 40 (2011) 21–26

Contents lists available at ScienceDirect

Solid State Nuclear Magnetic Resonance

journal homepage: www.elsevier.com/locate/ssnmr

Efficiency at high spinning frequencies of heteronuclear decoupling methods designed to quench rotary resonance

Markus Weingarth [a,b,c,1], Julien Trébosc [d], Jean-Paul Amoureux [d], Geoffrey Bodenhausen [a,b,c], Piotr Tekely [a,b,c,*]

[a] Ecole Normale Supérieure, Département de Chimie, 24 rue Lhomond, 75005 Paris, France
[b] Université Pierre-et-Marie Curie, Place Jussieu, 75005 Paris, France
[c] CNRS, UMR 7203, Département de Chimie, 24 rue Lhomond, 75005 Paris, France
[d] UCCS, CNRS 8181, Université de Lille-1, 59652 Villeneuve d'Ascq, France

ARTICLE INFO

Article history:
Received 30 November 2010
Received in revised form
17 March 2011
Available online 1 April 2011

Keywords:
Solid-state NMR
Heteronuclear decoupling
Fast magic-angle spinning (MAS)
Rotary resonance recoupling (R^3)
Phase-inverted supercycled sequence for attenuation of rotary resonance (PISSARRO)
High-phase two-pulse phase modulation (high-phase TPPM)

ABSTRACT

The performance of two recently developed heteronuclear decoupling schemes designed to quench rotary resonance, phase-inverted supercycled sequence for attenuation of rotary resonance (PISSARRO) and high-phase two-pulse phase modulation (high-phase TPPM), are probed at high spinning frequencies. High-phase TPPM may be useful at the $n=1$ rotary resonance condition while PISSARRO permits efficient decoupling over a broad commonly used range of rf amplitudes, even at very high spinning frequencies. New insights into the response of spin systems to both decoupling schemes have been gained. High-phase TPPM is sensitive to the offsets of remote protons, their chemical shift anisotropies, and the relative orientations of the heteronuclear dipolar and proton chemical shift tensors. Since PISSARRO is virtually immune against such effects, the method is especially suited for very high magnetic fields.

1. Introduction

Heteronuclear decoupling is of prime importance to obtain high-resolution NMR spectra of organic and biological solids containing dilute spins such as carbon-13. In polycrystalline or amorphous powders studied with fast magic-angle spinning (MAS), where flip-flop exchange between abundant protons slows down, the performance of continuous-wave (CW) decoupling is poor [1]. This drawback was overcome in the mid-1990s by substituting CW radio-frequency (rf) irradiation by phase-alternated irradiation [1], later called XiX [2], which offers a dramatic improvement in decoupling efficiency. This was followed by the popular two-pulse phase-modulated (TPPM) technique [3] and its variants [4–7], as well as a number of more sophisticated decoupling schemes [8–10].

Recent progress in MAS probe technology has opened the way to high spinning frequencies, which lead to efficient suppression of spinning sidebands at high magnetic fields and allow one to avoid line broadening in carbon-13 enriched systems due to *rotational resonance* (R^3) that occurs when an integer multiple of the spinning frequency ν_{rot} is roughly matched to the difference $\Delta\nu_{iso}$ between two isotropic chemical shifts ($n\nu_{rot}=\Delta\nu_{iso}$) [11]. Fast spinning can only be achieved with rotors of a small diameter that allow one to record spectra with as little as ~1 mg sample with good filling factors. However, in typical solids with strongly coupled spin networks, spinning frequencies $\nu_{rot}>30$ kHz bring new challenges for heteronuclear decoupling because it becomes difficult to avoid rotary resonance recoupling (R^3). This phenomenon has the most deleterious effects when the rf amplitude is a multiple of the spinning frequency ($\nu_1=n\nu_{rot}$) [12]. R^3 effects lead to a dramatic breakdown of the decoupling efficiency of standard decoupling schemes over a wide range of rf amplitudes [7,13–16]. Until recently, it was difficult to avoid R^3 effects at very fast spinning speeds without resorting to unreasonably high rf decoupling amplitudes.

To overcome this problem, a heteronuclear decoupling scheme dubbed phase-inverted supercycled sequence for attenuation of rotary resonance (PISSARRO) was developed [14]. This method turned out to be efficient over a wide range of rf amplitudes at $\nu_{rot}=30$ kHz and medium static fields (e.g., 400 MHz for protons at 9.4 T). Under these conditions, PISSARRO decoupling proved to be more effective in quenching rotary resonance effects in the vicinity of $n=2$ than established methods such as XiX [1,2], TPPM [3] or SPINAL-64 [17]. At high rf amplitudes, far from any R^3 conditions, PISSARRO has the same decoupling efficiency as XiX

* Corresponding author at: Ecole Normale Supérieure, Département de Chimie, 24 rue Lhomond, 75005 Paris, France.
E-mail address: Piotr.Tekely@ens.fr (P. Tekely).
[1] Current address: Utrecht University, Padualaan 8, 3584 CH Utrecht, The Netherlands.

0926-2040/$ - see front matter © 2011 Elsevier Inc. All rights reserved.
doi:10.1016/j.ssnmr.2011.03.004

and TPPM [14]. Moreover, it has been shown that at high spinning frequencies ($\nu_{rot}=60$ kHz) and high static fields (900 MHz for protons at 21T), PISSARRO decoupling remains remarkably efficient at commonly used rf amplitudes ($\nu_1 \sim 80$–100 kHz) [15,18]. Indeed, at these conditions, we have practically perfect quenching of rotary resonance at the $n=2$ condition under PISSARRO decoupling while such a performance remains unattainable for standard decoupling techniques, which require much higher rf amplitudes to reach the same efficiency [15,18]. This permits a reduction of the rf power dissipation in heat-sensitive samples such as hydrated proteins. Very recently, Paul et al. [19] introduced high-phase TPPM. This method is derived from the TPPM [3] scheme by increasing the phase shift to $\Delta\phi=150^\circ$, as opposed to $15^\circ < \Delta\phi < 30^\circ$ used in conventional

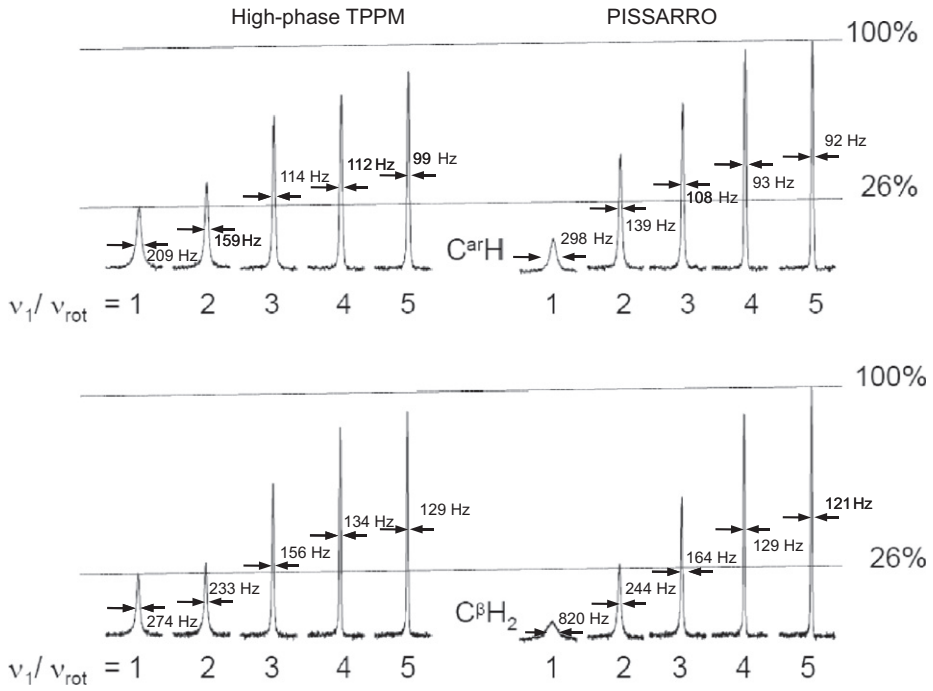

Fig. 1. Experimental comparison of the efficiency of heteronuclear decoupling for the $C^{\beta}H_2$ group in L-histidine with high-phase TPPM and PISSARRO (^{1}H carrier frequency placed on-resonance) and for one of the proton-carrying aromatic $C^{ar}H$ carbons (^{1}H carrier frequency 4.5 kHz off-resonance), at $\nu_{rot}=32$ kHz with different rf decoupling amplitudes ν_1 expressed in terms of the ratio ν_1/ν_{rot}. All spectra were recorded with 2 ms CP contact time, presaturation of ^{1}H (ten 90° pulses separated by 20 ms delays), $NS=8$ and 5 s delay between experiments and 28 ms acquisition time. No apodisation function was applied prior to the Fourier transformation.

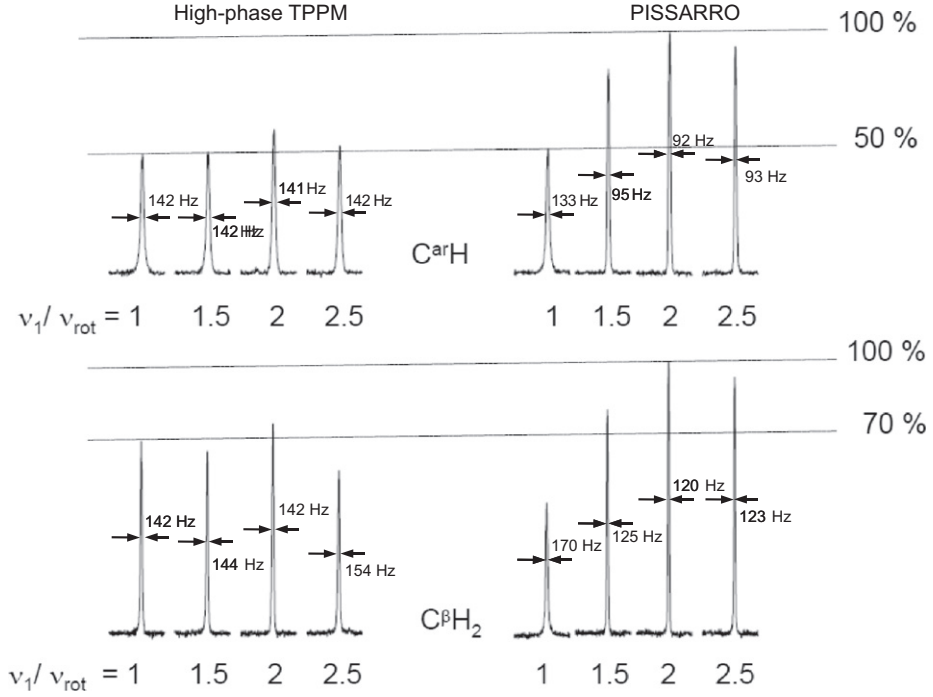

Fig. 2. Same as in Fig. 1, except that $\nu_{rot}=64$ kHz.

TPPM. At the same time, the flip angle β of the pulses must be proportional to the rf amplitude (as opposed to $\beta \sim \pi$ in conventional TPPM) [18]. Paul et al. [19,20] demonstrated that high-phase TPPM has a better performance than PISSARRO when $\nu_1 = \nu_{rot}$ ($n=1$) for $\nu_{rot}=20$ and 30 kHz.

In this work, we compare the decoupling performance of PISSARRO and high-phase TPPM at high magnetic field ($B_0=18.8$ T, 800 MHz for ^{1}H) for a wide range of rf amplitudes $15 \leq \nu_1 \leq 160$ kHz at two spinning frequencies $\nu_{rot}=32$ and 64 kHz. We also discuss why the spin systems respond in different ways to

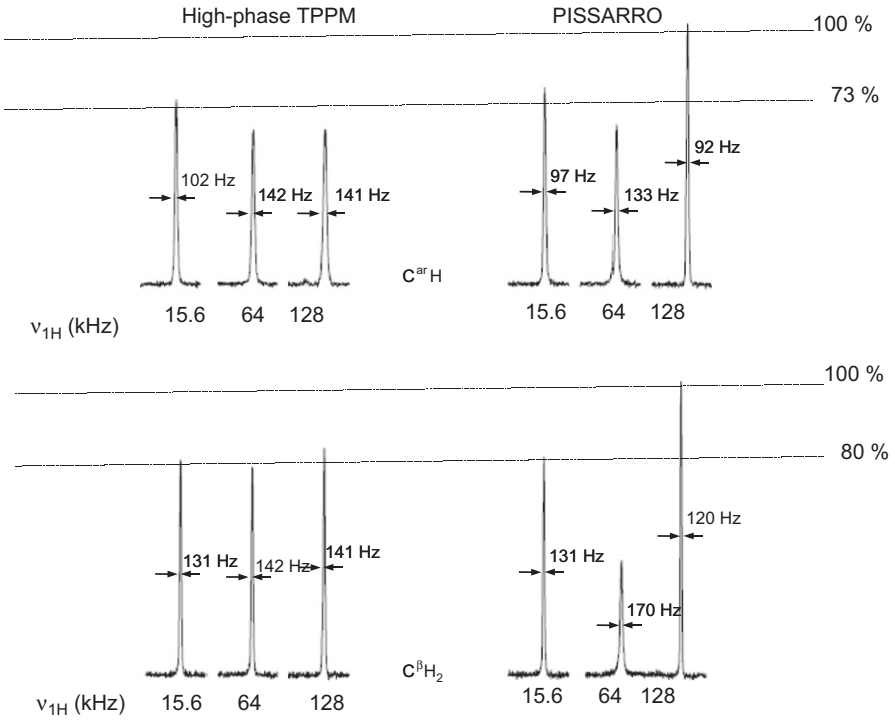

Fig. 3. Experimental comparison of the efficiency of heteronuclear decoupling in L-histidine at $\nu_{rot}=64$ kHz with a low rf amplitude $\nu_1=15.6$ kHz and high rf amplitudes $\nu_1=64$ or 128 kHz, i.e., with $n=\nu_1/\nu_{rot}=1$ or 2.

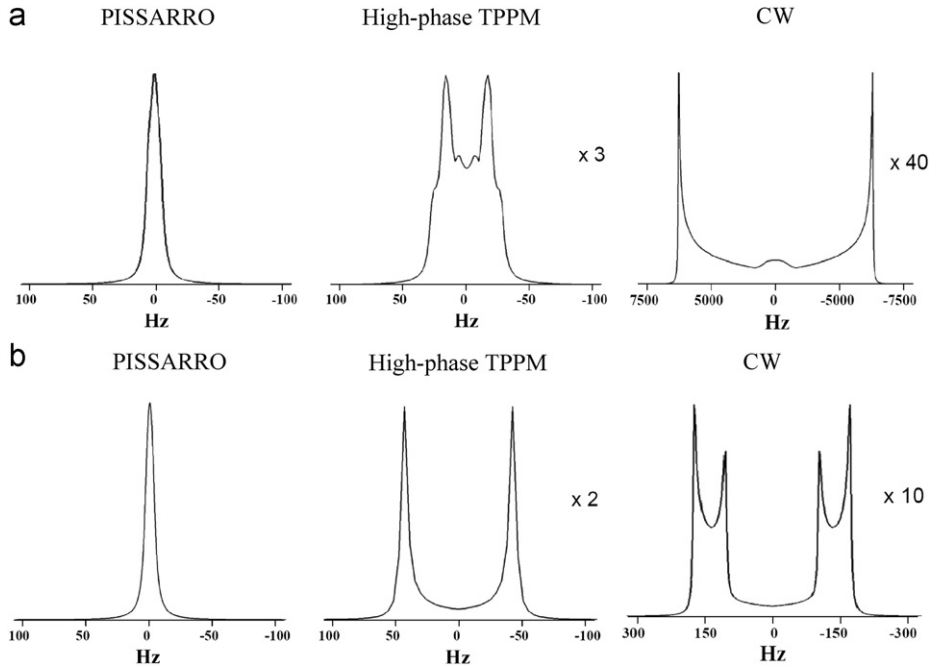

Fig. 4. Comparison of simulated ^{13}C line-shapes (with a line broadening of 5 Hz) for a two-spin ^{13}C-^{1}H system decoupled by PISSARRO, high-phase TPPM and CW irradiation, in a static magnetic field $B_0=18.8$ T, for $\nu_{rot}=64$ kHz with rf amplitudes (a) $\nu_1=128$ kHz (i.e., $n=\nu_1/\nu_{rot}=2$) and (b) $\nu_1=210$ kHz. The dipolar coupling constant was $d_{CH}=22.7$ kHz, the proton chemical shift anisotropy $\Delta\sigma_H=6.0$ ppm with $\eta=0$. The CSA and dipolar tensors were assumed to be coaxial. For PISSARRO the numerically optimized pulse widths were $\tau=0.1953\tau_{rot}$ in (a) and $\tau=0.9\tau_{rot}$ in (b), while for high-phase TPPM $\tau=4.5$ μs in (a) and $\tau=5.678$ μs in (b).

high-phase TPPM and to PISSARRO irradiation. The different responses can be understood with the help of numerical simulations.

2. Experimental

Spectra of a polycrystalline sample of uniformly ^{13}C-labeled L-histidine in a partially deprotonated form [21,22] were recorded on a Bruker AVANCE-II spectrometer operating at $B_0=18.8$ T and $\nu_{rot}=32$ or 64 kHz. The PISSARRO pulse sequence [14] consists in a train of forty pulses $[(\tau_x)(\tau_{-x})]_5[(\tau_{-x})(\tau_x)]_5[(\tau_y)(\tau_{-y})]_5[(\tau_{-y})(\tau_y)]_5$ organized in four blocks, each block containing five pulse pairs with opposite phases. The recommended pulse length τ for each spinning frequency ν_{rot} is $\tau=0.3\tau_{rot}$ for decoupling near the $n=1$ condition, $\tau=0.2\tau_{rot}$ for decoupling near the $n=2$ condition and $\tau=0.9\tau_{rot}$ or $1.1\tau_{rot}$ for high rf amplitudes (e.g., $\nu_1^H \gg 2\nu_{rot}$) [14]. These pulse durations can be used blindly, although an experimental optimization in the vicinity of the recommended lengths may provide minor improvement in decoupling efficiency. For low rf amplitudes, the pulse length τ should be optimized so that the nutation angle $\beta=2\pi\nu_1\tau$ is in the vicinity of a multiple of 2π [15]. In analogy to high-amplitude PISSARRO, half and full rotor periods should be avoided. For high-phase TPPM, the pulse duration was experimentally optimized in the range $4<\tau<6$ μs. Numerical simulations were carried out with SPINEVOLUTION [23], considering the 5-spin systems $C^{\alpha}H^{\alpha}H^{\beta1}H^{\beta2}H^{N}$ and $H^{\alpha}C^{\beta}H^{\beta1}H^{\beta2}H^{N}$ of L-serine using internuclear distances derived from the crystallographic structure. These spin systems are similar to $C^{\alpha}H^{\alpha}C^{\beta}H^{\beta1}H^{\beta2}$ or $C^{\alpha}H^{\alpha}H^{\beta1}H^{\beta2}H^{N1}H^{N2}H^{N+}$ of L-histidine and other common amino acids. For high-phase TPPM, the pulse duration was numerically optimized in the range $2<\tau<8$ μs.

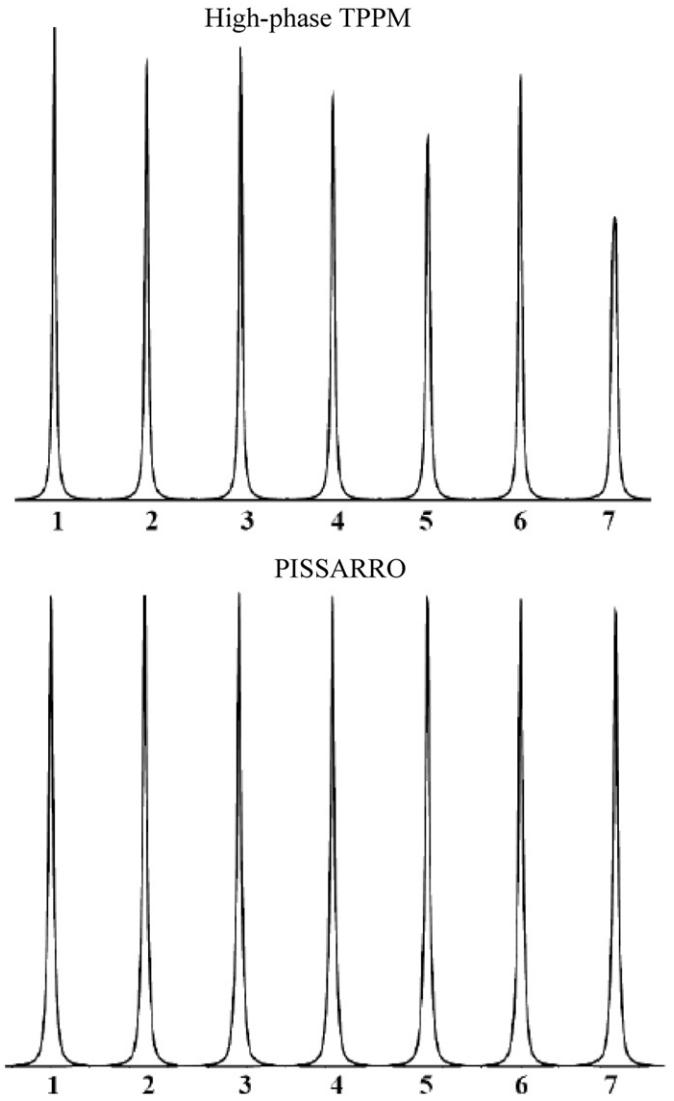

Fig. 5. Simulated $^{13}C^{\beta}$ line-shapes (with a line-broadening of 5 Hz) considering a spin cluster $C^{\beta}H^{\beta1}H^{\beta2}H^{\alpha}H^{N}$ in L-serine, for high-phase TPPM and PISSARRO decoupling, in a static magnetic field $B_0=18.8$ T, $\nu_{rot}=64$ kHz and $\nu_1=128$ kHz (i.e., $n=\nu_1/\nu_{rot}=2$) for different values $\Delta\sigma_H$ of the proton chemical shift anisotropy (with $\eta=0.3$) and different Euler angles (β,γ) describing the orientation of the $H^{\beta1}$ and $H^{\beta2}$ CSA tensors with respect to the principal axis systems of the dipolar $C^{\beta}H^{\beta1}$ and $C^{\beta}H^{\beta2}$ tensors: (1) $\Delta\sigma_H=6.0$ ppm; $\beta=76°$, 46°; $\gamma=77°$, 157°; (2) $\Delta\sigma_H=6.0$ ppm; $\beta=76°$, 1°; $\gamma=77°$, 157°; (3) $\Delta\sigma_H=6.0$ ppm; $\beta=76°$, 1°; $\gamma=77°$, 67°; (4) $\Delta\sigma_H=6.0$ ppm; $\beta=76°$, 1°; $\gamma=77°$, 8°; (5) $\Delta\sigma_H=6.0$ ppm; $\beta=36°$, 1°; $\gamma=77°$, 8°; (6) $\Delta\sigma_H=3.75$ ppm; $\beta=36°$, 8°; $\gamma=77°$, 8° and (7) $\Delta\sigma_H=10.0$ ppm; $\beta=36°$, 1°; $\gamma=77°$, 8°.

3. Results and discussion

3.1. Decoupling with high rf amplitudes

The performance of high-phase TPPM and PISSARRO at $\nu_{rot}=32$ and 64 kHz is compared in Figs. 1 and 2, respectively, for the $C^{\beta}H_2$ group of L-histidine (^{1}H carrier frequency placed on-resonance) and for one of the proton-carrying aromatic $C^{ar}H$ carbons (^{13}C at 136.3 ppm, ^{1}H carrier frequency 4.5 kHz off-resonance). A wide range

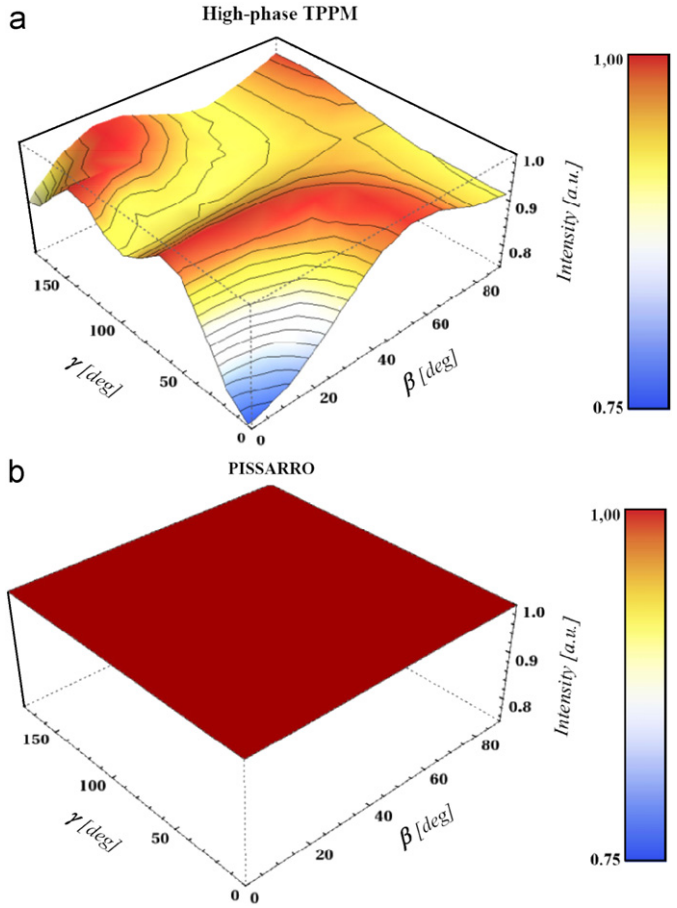

Fig. 6. Simulated $^{13}C^{\alpha}$ peak heights (normalized to the maximum peak height), considering a spin cluster $C^{\alpha}H^{\alpha}H^{\beta1}H^{\beta2}H^{N}$ in L-serine, for high-phase TPPM and PISSARRO decoupling, with $\Delta\sigma_H=6.0$ ppm as a function of the Euler angles (β,γ) describing the orientation of the H^{α} CSA tensor with respect to the principal axis system of the dipolar $C^{\alpha}H^{\alpha}$ tensor. All other parameters are as in Fig. 5.

of rf decoupling amplitudes was tested and expressed in terms of the ratio ν_1/ν_{rot}. In agreement with earlier observations [19,20], high-phase TPPM is more efficient than PISSARRO near $n=1$ for both $\nu_{rot}=32$ and 64 kHz. For both spinning frequencies, the best decoupling performance was observed with rf amplitudes $\nu_1 > 100$ kHz. At $\nu_{rot}=32$ kHz and $\nu_1=160$ kHz, PISSARRO yields gain in peak height of 10% or 14% for the $C^{\beta}H_2$ or $C^{ar}H$ groups, respectively. At $\nu_{rot}=64$ kHz, the best decoupling is observed for both methods at $\nu_1=2\nu_{rot}$ ($n=2$). High-phase TPPM yields $C^{\beta}H_2$ and $C^{ar}H$ signals with peak heights that are 78% and 59% of those obtained with PISSSARRO.

3.2. Low-amplitude decoupling

It has been shown recently that at very high spinning frequencies, it is possible to use low-power versions of CW, XiX, TPPM and PISSARRO decoupling [7,15,16,24–26]. At $\nu_{rot}=60$ kHz in a magnetic field $B_0=21$ T, PISSARRO with a very low rf amplitude $\nu_1=15$ kHz yielded virtually the same decoupling performance for both CH_3 and CH signals in alanine as with the highest accessible rf amplitudes [15]. On the other hand, the peak height of CH_2 in α-glycine [27] observed with $\nu_1=15$ kHz was 20% lower than could be obtained with $\nu_1=150$ kHz [15]. As shown in Fig. 3, in the case of the $C^{\beta}H_2$ signal of L-histidine recorded at $\nu_{rot}=64$ kHz, high-phase TPPM and PISSARRO provide the same performance with low-amplitude decoupling of 15 kHz while at $\nu_1=10$ kHz PISSARRO performs significantly better than high-phase TPPM (data not shown). In analogy to α-glycine, at $B_0=18.8$ T and $\nu_1=15$ kHz, both suffer from a 20% loss of peak height compared with high-power PISSARRO decoupling at $n=2$.

3.3. Effect of second-order cross-terms between C–H dipole–dipole and ^{1}H CSA interactions

As mentioned above, CW decoupling copes poorly with the fact that spin diffusion slows down at high spinning frequencies [1]. For on-resonance decoupling, the resulting spectral broadening is largely due to cross-terms between the heteronuclear dipolar and proton CSA interactions [28,29]. To investigate the role of these terms under PISSARRRO and high-phase TPPM, we have simulated the carbon-13 line-shape of an isolated C–H two-spin system at $\nu_{rot}=64$ kHz for two rf amplitudes $\nu_1=128$ kHz (i.e., at the $n=2$ condition) and $\nu_1=210$ kHz. We assume that both tensors are collinear, since this assumption leads to the largest second-order splitting [28]. Indeed, as shown in Fig. 4, we observe a broadened doublet for high-phase TPPM, which is reminiscent of the second-order splitting observed with CW decoupling [28,29]. This stands in contrast to the narrow carbon-13 line simulated for the same spin system with PISSARRO decoupling.

To probe further to what extent the dipolar/CSA cross-terms influence the efficiency of high-phase TPPM and PISSARRO decoupling at the $n=2$ condition, we carried out numerical simulations for the $C^{\alpha}H^{\alpha}H^{\beta 1}H^{\beta 2}H^{N}$ and $H^{\alpha}C^{\beta}H^{\beta 1}H^{\beta 2}H^{N}$ spin systems of L-serine. All intramolecular homo- and heteronuclear dipolar interactions were taken into account. Fig. 5 shows the carbon-13 line-shape of the $C^{\beta}H_2$ group, simulated for different Euler angles describing the orientation of the $H^{\beta 1}$- and $H^{\beta 2}$-CSA tensors in the principal axis systems of the dipolar $C^{\beta}H^{\beta 1}$ and $C^{\beta}H^{\beta 2}$ tensors [30] for three different values of the anisotropies of the proton chemical shifts. With PISSARRO decoupling, the amplitudes are nearly independent of the Euler angles, but significant variations in peak heights appear with high-phase TPPM as a function of these Euler angles. This is due to orientation-dependent second-order broadening that occurs with high-phase TPPM. Notably, larger proton chemical shift anisotropies lead to a decrease in the peak heights with high-phase TPPM, while only marginal effects occur with PISSARRO decoupling. Fig. 6 shows simulations of the carbon-13 peak height of the $C^{\alpha}H$ group as a function of the Euler angles describing the orientation of the H^{α}-CSA tensor in the principal axis system of the dipolar $C^{\alpha}H$ tensor [31,32]. Here again one observes substantial changes in peak heights for high-phase TPPM, in striking contrast with PISSARRO decoupling.

For completeness, Fig. 7 shows numerical simulations of the carbon-13 peak height of the $C^{\alpha}H$ group at the $n=2$ condition as a function of spinning frequency $40 < \nu_{rot} < 70$ kHz at static magnetic fields corresponding to ^{1}H resonance frequencies between 400 and 1000 MHz for the system $C^{\alpha}H^{\alpha}H^{\beta 1}H^{\beta 2}H^{N1}H^{N2}H^{N+}$ of L-histidine. Despite the limited number of protons, these simulations show that the efficiency of high-phase TPPM suffers from (i) the offsets of the remote protons, (ii) the chemical shift anisotropies of the protons, and (iii) the relative orientations of the CSA and dipolar tensors. By contrast, PISSARRO decoupling is practically immune to these parameters. A thorough discussion of the mechanism of quenching of rotary resonance recoupling effects by PISSARRO is presented elsewhere [18].

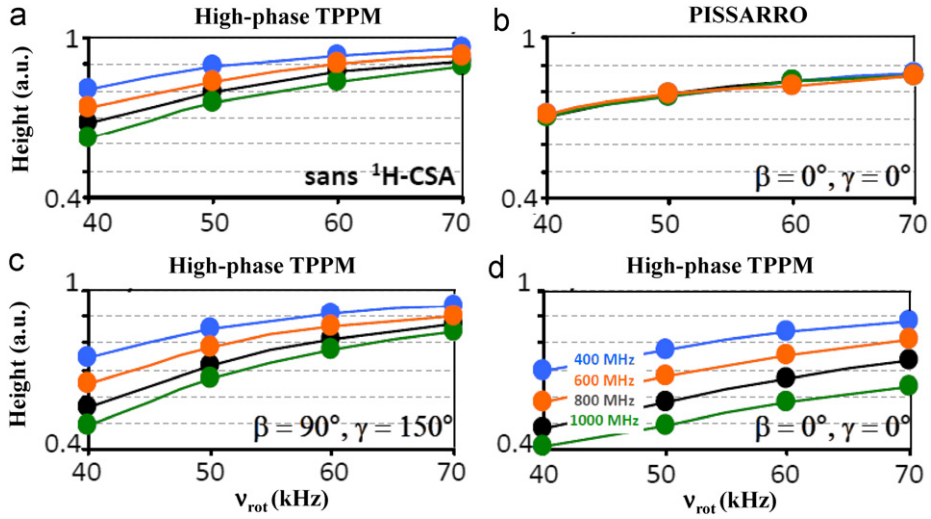

Fig. 7. Simulated $^{13}C^{\alpha}$ peak heights, considering a spin cluster $C^{\alpha}H^{\alpha}H^{\beta 1}H^{\beta 2}H^{N1}$ H^{N2} HN^{+} in L-histidine. (a, c and d) For high-phase TPPM and (b) for PISSARRO decoupling, as a function of ν_{rot} and B_0. The isotropic proton offsets were 0.0, 0.2, 0.2, 8.0, 8.0 and 4.0 ppm for H^{α}, $H^{\beta 1}$, $H^{\beta 2}$, H^{N1} , H^{N2}, H^{N+}, respectively. A chemical shift anisotropy $\Delta\sigma_H=4.0$ ppm with $\eta=0$ was assumed for each proton. In all cases the chemical shift anisotropy of C^{α} was assumed to be $\Delta\sigma_C=25.0$ ppm.

4. Conclusions

The decoupling efficiency of two recently proposed heteronuclear decoupling schemes designed to quench rotary resonance, PISSARRO and high-phase TPPM, was tested over a wide range of rf decoupling amplitudes. At very high spinning frequencies, high-phase TPPM may be useful at the $n=1$ rotary resonance condition while PISSARRO remains efficient over a broad commonly used range of rf decoupling amplitudes. Extensive numerical simulations reveal that high-phase TPPM is sensitive to the offsets of remote protons, their chemical shift anisotropies and the relative orientations of the tensors, all of which may be important at high static fields. Since PISSARRO is virtually immune to these effects, the method is especially suitable at very high magnetic fields.

Acknowledgments

Financial support from the Agence Nationale de la Recherche (ANR-09-BLAN-0111-01) and from the Fédération de Recherche (FR3050) Très Grands Equipements de Résonance Magnétique Nucléaire à Très Hauts Champs (TGE RMN THC) of the CNRS is gratefully acknowledged.

References

[1] P. Tekely, P. Palmas, D. Canet, J. Magn. Reson. A 107 (1994) 129–133.
[2] A. Detken, E.H. Hardy, M. Ernst, B.H. Meier, Chem. Phys. Lett. 356 (2002) 298–304.
[3] A.E. Bennett, C.M. Rienstra, M. Auger, K.V. Lakshli, R.G. Griffin, J. Chem. Phys. 103 (1995) 6951–6958.
[4] Z. Gan, R.R. Ernst, Solid State NMR 8 (1997) 153–159.
[5] K. Takegoshi, J. Mizokami, T. Terao, Chem. Phys. Lett. 341 (2001) 540–544.
[6] R.S. Thakur, N.D. Kurur, P.K. Madhu, Chem. Phys. Lett. 426 (2006) 459–463.
[7] M. Kotecha, N.P. Wickramasinghe, Y. Ishii, Magn. Reson. Chem. 45 (2007) S221–S230.
[8] M. Eden, M.H. Levitt, J. Chem. Phys. 111 (1999) 1511–1519.
[9] G. De Paëpe, P. Hodgkinson, L. Emsley, Chem. Phys. Lett. 376 (2003) 259–267.
[10] G. Gerbaud, F. Ziarelli, S. Caldarelli, Chem. Phys. Lett. 377 (2003) 1–5.
[11] D.P. Raleigh, M.H. Levitt, R.G. Griffin, Chem. Phys. Lett. 146 (1988) 71–76.
[12] T.G. Oas, R.G. Griffin, M.H. Levitt, J. Chem. Phys. 89 (1988) 692–695.
[13] M. Ernst, A. Samoson, B.H. Meier, J. Chem. Phys. 123 (2005) 064102–064110.
[14] M. Weingarth, P. Tekely, G. Bodenhausen, Chem. Phys. Lett. 466 (2008) 247–251.
[15] M. Weingarth, G. Bodenhausen, P. Tekely, J. Magn. Reson. 199 (2009) 238–241.
[16] S. Laage, J.R. Sachleben, S. Steuernagel, R. Pierattelli, G. Pintacuda, L. Emsley, J. Magn. Reson. 196 (2009) 133–141.
[17] B.M. Fung, A.K. Khitrin, K. Ermolaev, J. Magn. Reson. 142 (2000) 97–101.
[18] M. Weingarth, G. Bodenhausen, P. Tekely, Chem. Phys. Lett. 502 (2011) 259–265.
[19] S. Paul, V.S. Mithu, N.D. Kurur, P.K. Madhu, J. Magn. Reson. 203 (2009) 199–202.
[20] S. Paul, N.D. Kurur, P.K. Madhu, J. Magn. Reson. 207 (2010) 140–148.
[21] B. Henry, P. Tekely, J.J. Delpuech, J. Am. Chem. Soc. 124 (2002) 2025–2034.
[22] C. Gardiennet-Doucet, B. Henry, P. Tekely, Prog. NMR Spectrosc. 49 (2006) 129–149.
[23] M. Veshtort, R.G. Griffin, J. Magn. Reson. 178 (2006) 248–282.
[24] M. Ernst, A. Samoson, B.H. Meier, Chem. Phys. Lett. 348 (2001) 293–302.
[25] M. Ernst, A. Samoson, B.H. Meier, J. Magn. Reson. 163 (2003) 332–339.
[26] M. Weingarth, G. Bodenhausen, P. Tekely, Chem. Phys. Lett. 488 (2010) 10–16.
[27] M.J. Potrzebowski, P. Tekely, Y. Dusausoy, Solid State NMR 11 (1998) 253–257.
[28] M. Ernst, S. Bush, A.C. Kolbert, A. Pines, J. Chem. Phys. 105 (1996) 3387–3396.
[29] M. Ernst, H. Zimmermann, B.H. Meier, Chem. Phys. Lett. 317 (2000) 581–588.
[30] P. Tekely, J. Brondeau, K. Elbayed, A. Retournard, D. Canet, J. Magn. Reson. 80 (1988) 509–516.
[31] P. Tekely, F. Montigny, D. Canet, J.J. Delpuech, Chem. Phys. Lett. 175 (1990) 401–406.
[32] P. Palmas, C. Malveau, P. Tekely, D. Canet, Solid State NMR 13 (1998) 45–53.